

Table II. Bond Distances (Å) and Bond Angles (Deg) for  $V_{10}O_{26}^{4-}$ 

V(1)-O(1)	1.91 (2)	V(6)-O(3)	1.95 (2)
V(1)-O(11)	1.58 (1)	V(6)-O(7)	1.94 (1)
V(1)-O(14)	1.95 (2)	V(6)-O(23)	1.59 (1)
V(1)-O(15)	1.95 (1)	V(6)-O(25)	1.92 (1)
V(1)-O(21)	1.96 (2)	V(6)-O(26)	1.91 (1)
V(2)-O(19)	1.80 (1)	V(7)-O(3)	1.65 (2)
V(2)-O(21)	1.66 (2)	V(7)-O(4)	1.77 (2)
V(2)-O(22)	1.77 (1)	V(7)-O(17)	1.61 (2)
V(2)-O(24)	1.59 (2)	V(7)-O(19)	1.78 (2)
V(3)-O(1)	1.71 (2)	V(8)-O(2)	1.78 (1)
V(3)-O(2)	1.82 (1)	V(8)-O(18)	1.59 (2)
V(3)-O(16)	1.78 (1)	V(8)-O(22)	1.81 (1)
V(3)-O(20)	1.58 (2)	V(8)-O(26)	1.69 (2)
V(4)-O(5)	1.58 (2)	V(9)-O(8)	1.59 (2)
V(4)-O(6)	1.79 (2)	V(9)-O(12)	1.82 (1)
V(4)-O(12)	1.79 (1)	V(9)-O(16)	1.77 (1)
V(4)-O(14)	1.66 (2)	V(9)-O(25)	1.67 (2)
V(5)-O(4)	1.82 (2)	V(10)-O(6)	1.81 (2)
V(5)-O(9)	1.63 (2)	V(10)-O(7)	1.68 (2)
V(5)-O(13)	1.80 (2)	V(10)-O(10)	1.61 (2)
V(5)-O(15)	1.67 (2)	V(10)-O(13)	1.76 (2)
O(1)-V(1)-O(11)	105.4 (8)	O(3)-V(6)-O(7)	86.2 (6)
O(1)-V(1)-O(14)	85.3 (7)	O(3)-V(6)-O(23)	107.4 (8)
O(1)-V(1)-O(15)	150.6 (8)	O(3)-V(6)-O(25)	145.3 (7)
O(1)-V(1)-O(21)	86.8 (7)	O(3)-V(6)-O(26)	84.1 (7)
O(11)-V(1)-O(14)	109.6 (8)	O(7)-V(6)-O(23)	106.1 (8)
O(11)-V(1)-O(15)	84.1 (7)	O(7)-V(6)-O(25)	86.4 (6)
O(11)-V(1)-O(21)	107.3 (7)	O(7)-V(6)-O(26)	150.6 (7)
O(14)-V(1)-O(15)	84.1 (7)	O(23)-V(6)-O(25)	107.3 (8)
O(14)-V(1)-O(21)	143.1 (7)	O(23)-V(6)-O(26)	103.3 (8)
O(15)-V(1)-O(21)	85.4 (7)	O(25)-V(6)-O(26)	85.9 (7)
O(19)-V(2)-O(21)	109.5 (7)	O(3)-V(7)-O(4)	108.9 (7)
O(19)-V(2)-O(22)	111.4 (7)	O(3)-V(7)-O(17)	108.7 (8)
O(19)-V(2)-O(24)	108.6 (7)	O(3)-V(7)-O(19)	110.8 (7)
O(21)-V(2)-O(22)	109.6 (7)	O(4)-V(7)-O(17)	109.8 (8)
O(21)-V(2)-O(24)	110.4 (8)	O(4)-V(7)-O(19)	108.6 (7)
O(22)-V(2)-O(24)	107.3 (7)	O(17)-V(7)-O(19)	110.1 (8)
O(1)-V(3)-O(2)	108.0 (7)	O(2)-V(8)-O(18)	109.2 (7)
O(1)-V(3)-O(16)	110.1 (7)	O(2)-V(8)-O(22)	112.4 (6)
O(1)-V(3)-O(20)	109.6 (8)	O(2)-V(8)-O(26)	108.4 (7)
O(2)-V(3)-O(16)	112.6 (6)	O(18)-V(8)-O(22)	108.0 (8)
O(2)-V(3)-O(20)	107.6 (7)	O(18)-V(8)-O(26)	108.4 (9)
O(16)-V(3)-O(20)	109.0 (7)	O(22)-V(8)-O(26)	110.4 (7)
O(5)-V(4)-O(6)	107.1 (8)	O(8)-V(9)-O(12)	109.9 (7)
O(5)-V(4)-O(12)	107.8 (8)	O(8)-V(9)-O(16)	109.1 (8)
O(5)-V(4)-O(14)	111.2 (9)	O(8)-V(9)-O(25)	109.0 (8)
O(6)-V(4)-O(12)	112.2 (7)	O(12)-V(9)-O(16)	110.2 (7)
O(6)-V(4)-O(14)	109.9 (8)	O(12)-V(9)-O(25)	109.0 (7)
O(12)-V(4)-O(14)	108.6 (8)	O(16)-V(9)-O(25)	109.6 (7)
O(4)-V(5)-O(9)	108.2 (7)	O(6)-V(10)-O(7)	110.0 (7)
O(4)-V(5)-O(13)	110.9 (8)	O(6)-V(10)-O(10)	107.7 (8)
O(4)-V(5)-O(15)	109.4 (8)	O(6)-V(10)-O(13)	111.3 (8)
O(9)-V(5)-O(13)	107.6 (8)	O(7)-V(10)-O(10)	108.0 (8)
O(9)-V(5)-O(15)	109.3 (8)	O(7)-V(10)-O(13)	110.7 (8)
O(13)-V(5)-O(15)	111.3 (8)	O(10)-V(10)-O(13)	109.0 (8)
V(3)-O(1)-V(1)	165 (1)	V(5)-O(15)-V(1)	167 (1)
V(8)-O(2)-V(3)	123.7 (8)	V(9)-O(16)-V(3)	138.1 (9)
V(7)-O(3)-V(6)	173 (1)	V(7)-O(19)-V(2)	133.5 (9)
V(7)-O(4)-V(5)	122.7 (8)	V(2)-O(21)-V(1)	158 (1)
V(10)-O(6)-V(4)	126.3 (8)	V(8)-O(22)-V(2)	131.9 (8)
V(10)-O(7)-V(6)	155 (1)	V(9)-O(25)-V(6)	165 (1)
V(9)-O(12)-V(4)	123.6 (8)	V(8)-O(26)-V(6)	178 (1)
V(10)-O(13)-V(5)	138 (1)		
V(4)-O(14)-V(1)	167 (1)		

structure (as in  $V_{18}O_{48}^{12-2}$ ) by the addition of the two V(IV) tetragonal pyramids.

**Registry No.**  $[(C_2H_5)_4N]_4V_{10}O_{26} \cdot H_2O$ , 79482-74-9.

**Supplementary Material Available:** Tables of bond distances and angles in the tetraethylammonium ions (Table III), structure factors, and thermal parameters (47 pages). Ordering information is given on any current masthead page.

Contribution from the Department of Chemistry, Texas A&M University, College Station, Texas 77843

### Crystal and Molecular Structure of Tetrakis(trifluoroacetato)bis(dimethyl- $d_6$ sulfoxide)dirhodium(II): A Structural Deuterium Isotope Effect in an Oxygen-Bonded Sulfoxide Adduct

F. Albert Cotton\* and Timothy R. Felthouse

Received June 25, 1981

Although the preference of platinum group metal ions to bind dimethyl sulfoxide ( $Me_2SO$ ) through the sulfur atom was recognized<sup>1</sup> over 20 years ago, more recent studies have found that this affinity may be offset by steric<sup>2-4</sup> or electronic<sup>5,6</sup> factors imparted to the metal ion through the coordinated ligand atoms. Thus, steric effects favor oxygen-bonded  $Me_2SO$  ligands in the crowded four-coordinate  $[M-(Ph_2PCH_2CH_2PPh_2)(Me_2SO)Cl]^+$  complexes<sup>4</sup> ( $M = Pd^{II}$ ,  $Pt^{II}$ ), electronic effects govern oxygen coordination of  $Me_2SO$  in  $Rh_2(O_2CCF_3)_4(Me_2SO)_2$ ,<sup>6</sup> while both steric and electronic factors play a role in the mixed oxygen- and sulfur-bonded complexes of  $Pd(Me_2SO)_4^{2+}$ ,<sup>3</sup>  $Rh(Me_2SO)_3Cl_3$ ,<sup>7</sup> and  $Ru(Me_2SO)_4Cl_2$ .<sup>8</sup>

During our previous work<sup>6</sup> involving the correlation of S-O bond lengths with  $\nu(S-O)$  frequencies in  $Me_2SO$  adducts of  $Rh_2(O_2CR)_4$  compounds, the perdeuterated compound  $Rh_2(O_2CCF_3)_4(Me_2SO-d_6)_2$  was prepared in order to aid in the assignment of the infrared spectrum of the  $Me_2SO$  adduct. Earlier studies<sup>9,10</sup> have noted that the advantage derived from recording the infrared spectra of both  $Me_2SO$  and  $Me_2SO-d_6$  compounds stems from the near degeneracy of the S-O stretching and methyl rocking vibrations in the normal  $Me_2SO$  complex while in the  $Me_2SO-d_6$  analogue these vibrations are well separated. Since the preparation of  $Rh_2(O_2CCF_3)_4(Me_2SO-d_6)_2$  afforded a crystalline product, several of the crystals were examined on an X-ray diffractometer. Unexpectedly, all of the crystals examined possessed a triclinic cell which was not the same as that for the corresponding  $Rh_2(O_2CCF_3)_4(Me_2SO)_2$  complex.<sup>6</sup>

In this paper we describe the structure of the  $Me_2SO-d_6$  adduct of  $Rh_2(O_2CCF_3)_4$ , which has been refined with the inclusion of all deuterium atoms. This structure is compared to that of the undeuterated adduct<sup>6</sup> which has been further refined with the inclusion of all hydrogen atoms. The two structures represent, to our knowledge, the first example of a crystal packing modification in a transition-metal complex effected solely by the substitution of deuterium for hydrogen.

### Experimental Section

Rhodium(II) trifluoroacetate was prepared by the procedure given by Kitchens and Bear<sup>11</sup> and converted to the anhydrous form by heating at 150 °C for 30 min. Glistening dark blue irregularly shaped crystals of  $Rh_2(O_2CCF_3)_4(Me_2SO-d_6)_2$  were obtained directly upon evaporation of a 1:1 mixture of benzene-chloroform containing  $Rh_2(O_2CCF_3)_4$  and excess practical grade Bio-Rad  $Me_2SO-d_6$ .

- (1) Cotton, F. A.; Francis, R. *J. Am. Chem. Soc.* **1960**, *82*, 2986.
- (2) Wayland, B. B.; Schramm, R. F. *Inorg. Chem.* **1969**, *8*, 971.
- (3) Price, J. H.; Williamson, A. N.; Schramm, R. F.; Wayland, B. B. *Inorg. Chem.* **1972**, *11*, 1280.
- (4) Davies, J. A.; Hartley, F. R.; Murray, S. G. *J. Chem. Soc., Dalton Trans.* **1979**, 1705.
- (5) Cotton, F. A.; Felthouse, T. R. *Inorg. Chem.* **1980**, *19*, 323.
- (6) Cotton, F. A.; Felthouse, T. R. *Inorg. Chem.* **1980**, *19*, 2347.
- (7) Sokol, V. I.; Porai-Koshits, M. A. *Sov. J. Coord. Chem.* **1975**, *1*, 476.
- (8) Mercer, A.; Trotter, J. *J. Chem. Soc., Dalton Trans.* **1975**, 2480.
- (9) Cotton, F. A.; Francis, R.; Horrocks, W. D., Jr. *J. Phys. Chem.* **1960**, *64*, 1534.
- (10) Horrocks, W. D., Jr.; Cotton, F. A. *Spectrochim. Acta* **1961**, *17*, 134.
- (11) Kitchens, J.; Bear, J. L. *Thermochim. Acta* **1970**, *1*, 537.

**X-ray Crystallography. Collection of Data.** A crystal of  $\text{Rh}_2(\text{O}_2\text{CCF}_3)_4(\text{Me}_2\text{SO}-d_6)_2$  having the dimensions  $0.10 \times 0.15 \times 0.35$  mm was mounted on a glass fiber with epoxy cement and examined on an Enraf-Nonius CAD-4 diffractometer using a random search procedure. A total of 25 reflections were located, centered, and indexed producing a triclinic cell which did not transform to a cell of higher symmetry upon application of a Delaunay reduction. Several other crystals were examined and none produced a cell identical with the one for  $\text{Rh}_2(\text{O}_2\text{CCF}_3)_4(\text{Me}_2\text{SO})_2$ .<sup>6</sup> The final cell constants were obtained from 25 reflections with  $17^\circ < 2\theta < 33^\circ$ . Crystal data for  $\text{Rh}_2(\text{O}_2\text{CCF}_3)_4(\text{Me}_2\text{SO}-d_6)_2$ ,  $\text{Rh}_2\text{S}_2\text{F}_{12}\text{O}_{10}\text{C}_{12}\text{D}_{12}$ , are as follows: triclinic,  $a = 9.699$  (1) Å,  $b = 14.664$  (2) Å,  $c = 8.614$  (2) Å,  $\alpha = 91.42$  (1)°,  $\beta = 91.24$  (1)°,  $\gamma = 83.32$  (1)°,  $V = 1216.2$  (5) Å<sup>3</sup>;  $Z = 2$ ; mol wt 826.21;  $d_c = 2.26$  g cm<sup>-3</sup>;  $F(000) \mu(\text{Mo K}\alpha) 788$ ;  $\mu(\text{MoK}\alpha) = 16.388$  cm<sup>-1</sup>; space group  $P\bar{1}$ .

Intensity data were collected for 4281 unique reflections having indices  $+h, \pm k, \pm l$  out to  $2\theta = 50^\circ$ . A scan width of  $\Delta\omega = (0.65 + 0.35 \tan \theta)^\circ$  was used and other data collection parameters were identical with those cited previously.<sup>12</sup> No crystal decomposition was noted during the 34 h of X-ray exposure time. The formulas used to derive the intensity and its standard deviation have been given before.<sup>13</sup>

Corrections for Lorentz and polarization effects were applied to the data as well as a correction for absorption. The absorption correction was based on an empirical method using  $\Psi$  scans ( $\Psi = 0-360^\circ$  every  $10^\circ$ ) for  $\chi$  values near  $90^\circ$ . Nine sets of  $\Psi$  scans were collected for 420, 42 $\bar{1}$ , 410, 411, 31 $\bar{1}$ , 311, 22 $\bar{1}$ , 43 $\bar{1}$ , and 75 $\bar{1}$  and averaged to yield maximum, minimum, and average transmission values of 1.00, 0.93, and 0.97, respectively.

**Structure Solution and Refinement.**<sup>14</sup>  $\text{Rh}_2(\text{O}_2\text{CCF}_3)_4(\text{Me}_2\text{SO}-d_6)_2$ . The positions of the two independent Rh atoms were derived from a three-dimensional Patterson function. Four cycles of least-squares refinement of these positions with isotropic temperature factors and a scale factor produced residuals of

$$R_1 = \sum |F_o| - |F_c| / \sum |F_o| = 0.36$$

$$R_2 = [\sum w(|F_o| - |F_c|)^2 / \sum w|F_o|^2]^{1/2} = 0.46$$

A combination of difference Fourier syntheses followed by least-squares refinement located all 38 nondeuterium atoms in the asymmetric unit. Anisotropic temperature factors were assigned to Rh, S, F, O, and C atoms, and the structure was further refined. A difference Fourier synthesis now revealed the positions of 10 of the 12 deuterium atoms, and these were refined with fixed isotropic thermal parameters of  $7.0$  Å<sup>2</sup>. The positions of D(202) and D(203) were calculated by assuming an idealized tetrahedral geometry about C(20) with C-D distances of  $0.95$  Å. The entire structure was then refined to convergence with 50 atoms, 373 variable parameters, and 3371 data with  $I > 3\sigma(I)$ . Final agreement factors were  $R_1 = 0.025$  and  $R_2 = 0.035$  with the esd of an observation of unit weight having a value of 1.058. In the final least-squares cycle, the largest shift/error ratio for a variable parameter was 0.42. A final difference Fourier map showed the largest peak equal to  $0.32 e \text{ \AA}^{-3}$ . A table of observed and calculated structure factor amplitudes with  $I > 3\sigma(I)$  is available.<sup>15</sup>

$\text{Rh}_2(\text{O}_2\text{CCF}_3)_4(\text{Me}_2\text{SO})_2$ . This structure has been reported before<sup>6</sup> with all 19 nonhydrogen atoms included in the refinement producing final residuals of  $R_1 = 0.042$  and  $R_2 = 0.070$  for 172 variable parameters with 1984 data having  $I > 3\sigma(I)$ . From the final difference Fourier map, the positions of the six methyl hydrogen atoms were located and the entire structure was refined with isotropic thermal parameters for all hydrogen atoms. Final residuals of  $R_1 = 0.038$  and  $R_2 = 0.060$  were obtained with 25 atoms included in the refinement, 196 variable parameters, and 1984 data. The final esd of an observation of unit weight was 1.651. The largest peak in the final difference Fourier map was  $0.52 e \text{ \AA}^{-3}$ , and the seven highest peaks were all associated with the fluorine atoms indicative of a very small amount of disorder about the threefold axes of the  $\text{CF}_3$  groups. A listing of observed and calculated structure factor amplitudes for this refinement is available.<sup>15</sup>

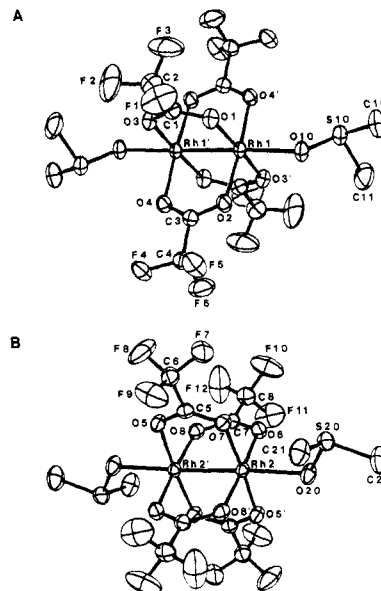


**Figure 1.** View of the two independent molecules (A and B) in  $\text{Rh}_2(\text{O}_2\text{CCF}_3)_4(\text{Me}_2\text{SO}-d_6)_2$  with thermal ellipsoids scaled so as to enclose 40% of their electron density. Each molecule resides on a crystallographic center of inversion located at the midpoint of the Rh-Rh bond.

## Results and Discussion

Table I records the final positional and thermal parameters for the two independent dinuclear molecules of  $\text{Rh}_2(\text{O}_2\text{CCF}_3)_4(\text{Me}_2\text{SO}-d_6)_2$ , and Table II presents the nondeuterium bond distances and angles. Bond distances and angles involving the deuterium atoms appear in Table IIA.<sup>15</sup> The final positional and anisotropic thermal parameters for  $\text{Rh}_2(\text{O}_2\text{CCF}_3)_4(\text{Me}_2\text{SO})_2$  are given in Table III,<sup>15</sup> and Table IV<sup>15</sup> includes the bond distances and angles for this compound. Least-squares planes for the two structures are compiled in Table V.<sup>15</sup>

**Description of the Structures.** Two crystallographically unique dinuclear molecules are contained in the unit cell of  $\text{Rh}_2(\text{O}_2\text{CCF}_3)_4(\text{Me}_2\text{SO}-d_6)_2$ , and these are shown in Figure 1. Each molecule resides on a crystallographic center of inversion with Rh-Rh distances of 2.409 (1) and 2.407 (1) Å for molecules A and B, respectively. The Rh-Rh bond lengths are within the range found for  $\text{Rh}_2(\text{O}_2\text{CCF}_3)_4\text{L}_2$  complexes, which extends from 2.399 (1) Å ( $\text{L} = \text{Me}_2\text{SO}_2$ <sup>12</sup>) to 2.486 (1) Å ( $\text{L} = \text{PPh}_3$ <sup>16</sup>). The rhodium atoms exhibit distorted octahedral geometries typical of  $\text{M}_2(\text{O}_2\text{CR})_4\text{L}_2$  complexes<sup>17</sup> with axial Rh and  $\text{O}(\text{Me}_2\text{SO}-d_6)$  atoms and equatorial trifluoroacetate oxygen atoms. The Rh atoms in A and B are displaced 0.076 and 0.075 Å, respectively, out of the equatorial oxygen atom plane (Table V<sup>15</sup>) toward the axial ligands. The  $\text{Me}_2\text{SO}-d_6$  molecules coordinate through their oxygen atoms at slightly (0.029 Å) different distances in molecules A and B, but this difference has essentially no effect on the Rh-Rh distances due to the weakly bonding character of axial oxygen donor ligands.<sup>18</sup> As seen in Figure 2, the two dinuclear molecules pack in a zigzag fashion in the unit cell forming a  $55^\circ$  dihedral angle between the equatorial carboxylate oxygen atom planes.

The structure of  $\text{Rh}_2(\text{O}_2\text{CCF}_3)_4(\text{Me}_2\text{SO})_2$  has been described before,<sup>6</sup> and inclusion of the methyl hydrogen atoms into the refinement leads to significant changes (i.e.,  $>3\sigma$ ) only in the S-C(6) bond length and the O(5)-S-C(5) and F(4)-

(12) Cotton, F. A.; Felthouse, T. R. *Inorg. Chem.* **1981**, *20*, 2703.

(13) Bino, A.; Cotton, F. A.; Fanwick, P. E. *Inorg. Chem.* **1979**, *18*, 3558.

(14) All crystallographic computing was done on a PDP 11/45 computer at the Molecular Structure Corp., College Station, TX, with the Enraf-Nonius structure determination package with local modifications.

(15) Supplementary material.

(16) Cotton, F. A.; Felthouse, T. R.; Klein, S. *Inorg. Chem.* **1981**, *20*, 3037.

(17) For a survey of structural data on  $\text{M}_2(\text{O}_2\text{CR})_4\text{L}_2$  complexes, see: Koh, Y. B.; Christoph, G. G. *Inorg. Chem.* **1979**, *18*, 1122.

(18) Bursten, B. E.; Cotton, F. A. *Inorg. Chem.* **1981**, *20*, 3042.

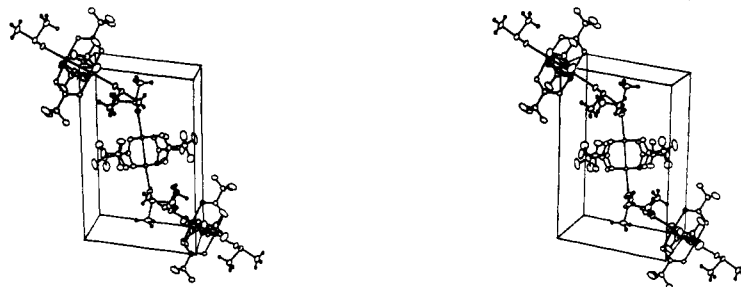


**Figure 2.** Stereoview of the unit cell contents in  $\text{Rh}_2(\text{O}_2\text{CCF}_3)_4(\text{Me}_2\text{SO}-d_6)_2$  as seen down the  $c$  axis with the  $a$  axis horizontal and the  $b$  axis vertical. The origin is located in the upper front left corner. Vibrational ellipsoids are drawn at the 20% probability level except the deuterium atoms which were made arbitrarily small for clarity. Molecule A is shown in the center of the cell with two dinuclear units of molecule B residing about (0, 0, 0) and (1, 1, 1).

C(4)–F(6) bond angles. Apart from the different number of independent dinuclear molecules per unit cell, the  $\text{Me}_2\text{SO}$  ( $Z = 1$ ) and  $\text{Me}_2\text{SO}-d_6$  ( $Z = 2$ ) adducts of  $\text{Rh}_2(\text{O}_2\text{CCF}_3)_4$  have Rh–Rh distances which differ by more than 0.01 Å, a change that must be attributed solely to differences in packing forces in the two structures. The molecular packing is influenced by the orientation of the sulfoxide ligands with respect to the  $\text{RhO}_4$  “face” of the  $\text{Rh}_2(\text{O}_2\text{CCF}_3)_4$  molecules. Figure 3 displays the orientations adopted by the  $\text{Me}_2\text{SO}$  ligands in  $\text{Rh}_2(\text{O}_2\text{CCF}_3)_4(\text{Me}_2\text{SO}-d_6)_2$  (A and B) and  $\text{Rh}_2(\text{O}_2\text{CCF}_3)_4(\text{Me}_2\text{SO})_2$  (C). Particularly noteworthy in these two structures is the Rh–O–S angle. In the  $\text{Me}_2\text{SO}-d_6$  adduct it has values of 120.1 (2) and 120.0 (2)° for molecules A and B, while in the  $\text{Me}_2\text{SO}$  adduct it increases to 132.3 (2)°. In contrast to the zigzag pattern of molecular packing in  $\text{Rh}_2(\text{O}_2\text{CCF}_3)_4(\text{Me}_2\text{SO}-d_6)_2$ , the  $\text{Me}_2\text{SO}$  analogue packs with all Rh–Rh vectors and carboxylate oxygen equatorial planes parallel, and this arrangement of dinuclear molecules is shown in Figure 4.

The geometries of the  $\text{Me}_2\text{SO}$  and  $\text{Me}_2\text{SO}-d_6$  ligands are closely similar with minor differences that cannot be attributed solely to the effects of deuteration since the packing arrangements differ. The S–O and mean S–C bond lengths in the  $\text{Me}_2\text{SO}$  ligand are 1.517 (3) and 1.778 (7) Å, respectively, while the corresponding bond lengths in the  $\text{Me}_2\text{SO}-d_6$  molecules average 1.516 (3) and 1.769 (7) Å. These S–O bond lengths are practically identical with the S–O distance of 1.513 (5) Å found in  $\text{Me}_2\text{SO}$  itself.<sup>19</sup> However, these distances contrast sharply with the S–O bond length found in S-bonded complexes such as  $\text{Rh}_2(\text{O}_2\text{CCH}_3)_4(\text{Me}_2\text{SO})_2$ ,<sup>5</sup> which decreases by about 0.40 Å to 1.477 (5) Å. This is consistent with an increase in the S–O bond order. Angular variations between the normal and deuterated  $\text{Me}_2\text{SO}$  adducts of  $\text{Rh}_2(\text{O}_2\text{CCF}_3)_4$  are somewhat more pronounced with average O–S–C and C–S–C angles in  $\text{Me}_2\text{SO}$  having values of 107.0 (3) and 97.7 (3)° while the corresponding mean angles in the deuterated molecule are 104.9 (3) and 99.4 (4)°.

**Structural Isotope Effects.** The two structures described here represent an unusual example of a packing modification in a transition-metal complex which is associated with the substitution of  $\text{CD}_3$  for  $\text{CH}_3$  groups in the axial sulfoxide ligands. The scope of the present work, however, does not rule out the possibility that both crystal forms exist for the normal and deuterated  $\text{Me}_2\text{SO}$  adducts of  $\text{Rh}_2(\text{O}_2\text{CCF}_3)_4$ .

A survey of the literature<sup>20</sup> on the structures of normal and deuterated forms of the same compound reveals relatively few examples of space group changes induced by isotopic substitution. Structural differences between compounds that differ only in whether they contain protium or deuterium may be attributed to variations in the zero-point vibrational amplitudes

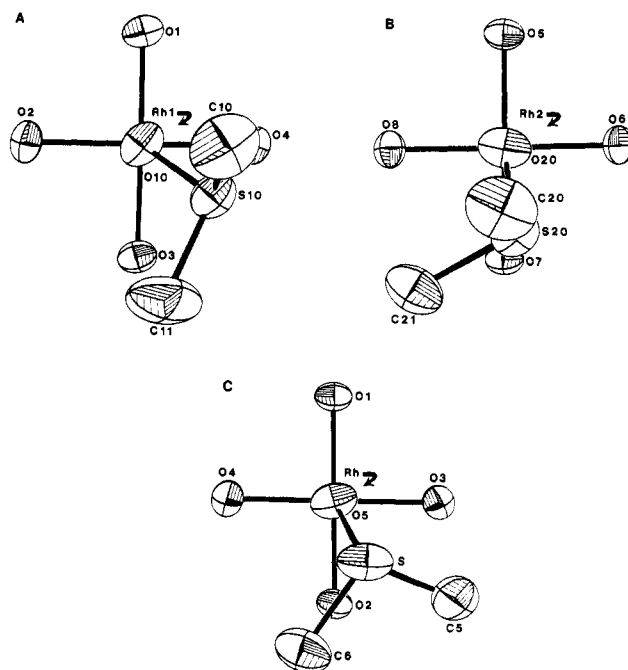


**Figure 3.** Orientations of the  $\text{Me}_2\text{SO}$  molecules relative to the  $\text{RhO}_4$  moieties in  $\text{Rh}_2(\text{O}_2\text{CCF}_3)_4(\text{Me}_2\text{SO}-d_6)_2$  (molecules A and B) and  $\text{Rh}_2(\text{O}_2\text{CCF}_3)_4(\text{Me}_2\text{SO})_2$  (C). Thermal ellipsoids are drawn at the 50% probability level. Primed atoms are not specifically labeled but are readily derived by comparison with the atom labeling scheme in Figure 1.

of protium and deuterium.<sup>21</sup> In an ionic crystal such as hydrazinium hydrogen oxalate,<sup>22</sup> the effect of isotopic substitution is to switch from the centrosymmetric space group  $P2_1/m$  containing a symmetrical hydrogen bond to the acentric space group  $P2_1$  containing a disordered arrangement of deuterium atoms.

More pertinent to our results is the work of McBride et al.,<sup>23</sup> who studied the effect on the crystal structure of azobis(isobutyronitrile),  $\text{NCC}(\text{CH}_3)_2\text{NNC}(\text{CH}_3)_2\text{CN}$ , of changing from  $\text{CH}_3$  to  $\text{CD}_3$ . The deuterio and protio compounds each form both monoclinic and triclinic crystals, and in each case the unit cell for the deuterated compound had a cell volume 0.2–0.3% smaller than that of the protio compound. This suggests that a  $\text{CD}_3$  group has a smaller van der Waals radius than a  $\text{CH}_3$  group, but only to a very slight extent. In this case the methyl groups make up a rather substantial part (ca. 30%) of the volume of the molecule, and still, the effect is almost negligible. There are also some other types of evidence<sup>24</sup> that the effective

(19) Thomas, R.; Shoemaker, C. B.; Eriks, K. *Acta Crystallogr.* **1966**, *21*, 12.  
 (20) We thank Dr. S. Bellard for providing a listing of these structures.

(21) Ubbelohde, A. R. *Trans. Faraday Soc.* **1935**, *32*, 525.  
 (22) Thomas, J. O. *Acta Crystallogr., Sect. B* **1973**, *B29*, 1767.  
 (23) Jaffe, A. B.; Malament, D. S.; Slisz, E. P.; McBride, J. M. *J. Am. Chem. Soc.* **1972**, *94*, 8515.

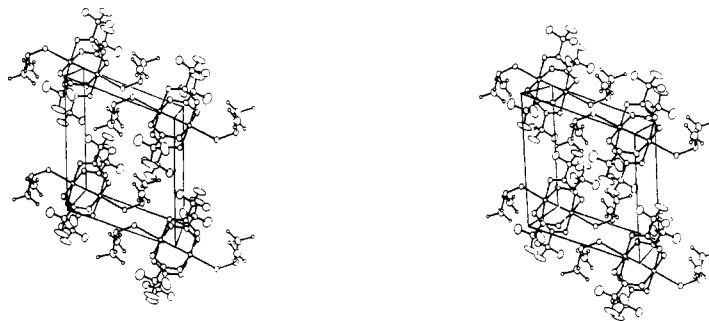
**Table I.** Positional and Thermal Parameters and Their Estimated Standard Deviations for  $\text{Rh}_2(\text{O}_2\text{CCF}_3)_4(\text{Me}_2\text{SO}-d_6)_2^{a,b}$ 

atom	x	y	z	$B_{11}$	$B_{22}$	$B_{33}$	$B_{12}$	$B_{13}$	$B_{23}$
Rh(1)	0.48289 (3)	0.42146 (2)	0.52304 (3)	2.82 (1)	1.91 (1)	2.24 (1)	-0.705 (9)	0.43 (1)	-0.028 (9)
Rh(2)	0.10688 (3)	0.03253 (2)	0.02474 (3)	1.95 (1)	2.31 (1)	2.28 (1)	-0.679 (9)	0.078 (9)	-0.094 (9)
S(10)	0.4082 (1)	0.23932 (7)	0.7062 (1)	4.31 (5)	3.09 (4)	3.22 (4)	-1.12 (4)	0.68 (4)	0.25 (3)
S(20)	0.3462 (1)	0.13405 (8)	0.2100 (1)	3.41 (4)	4.17 (5)	3.64 (4)	-1.35 (4)	-0.54 (4)	0.18 (4)
F(1)	0.8868 (4)	0.3468 (3)	0.2350 (4)	5.9 (2)	10.3 (2)	8.5 (2)	1.0 (2)	2.3 (1)	-4.3 (2)
F(2)	0.9452 (3)	0.4770 (3)	0.2724 (5)	6.3 (1)	8.5 (2)	14.9 (2)	-0.3 (1)	6.5 (1)	2.3 (2)
F(3)	0.9669 (3)	0.3809 (3)	0.4498 (4)	4.4 (1)	15.5 (3)	7.3 (2)	2.5 (2)	-0.6 (1)	1.3 (2)
F(4)	0.3496 (3)	0.5401 (2)	-0.0297 (3)	5.9 (1)	4.3 (1)	3.04 (9)	-0.5 (1)	-0.4 (1)	0.72 (9)
F(5)	0.3552 (4)	0.3970 (2)	0.0021 (3)	10.2 (2)	3.5 (1)	3.7 (1)	-1.2 (1)	-0.9 (1)	-0.9 (1)
F(6)	0.1835 (3)	0.4888 (3)	0.0846 (3)	3.6 (1)	12.2 (2)	5.2 (1)	-1.9 (1)	-0.4 (1)	0.4 (2)
F(7)	-0.0443 (3)	0.1059 (2)	0.5279 (3)	4.9 (1)	8.6 (2)	3.1 (1)	-0.6 (1)	-0.1 (1)	-1.7 (1)
F(8)	-0.2244 (3)	0.0423 (3)	0.4888 (3)	8.5 (2)	10.8 (2)	4.7 (1)	-4.7 (1)	3.5 (1)	-1.9 (1)
F(9)	-0.2132 (4)	0.1749 (2)	0.4015 (4)	9.6 (2)	6.7 (2)	5.2 (1)	4.3 (1)	-0.7 (1)	-1.6 (1)
F(10)	0.2535 (4)	-0.2405 (2)	0.2830 (4)	12.3 (2)	5.7 (2)	6.1 (2)	2.4 (2)	-3.0 (2)	0.7 (1)
F(11)	0.2770 (4)	-0.2779 (2)	0.0528 (4)	9.9 (2)	5.3 (2)	8.1 (2)	2.8 (2)	2.4 (2)	0.2 (1)
F(12)	0.1011 (4)	-0.3069 (2)	0.1682 (6)	5.8 (2)	5.4 (1)	24.5 (4)	-1.1 (1)	-1.5 (2)	7.3 (2)
O(1)	0.6743 (3)	0.3835 (2)	0.4352 (3)	3.5 (1)	2.8 (1)	3.8 (1)	-0.3 (1)	1.0 (1)	-0.1 (1)
O(2)	0.3987 (3)	0.4162 (2)	0.3061 (3)	4.5 (1)	2.7 (1)	2.7 (1)	-1.39 (9)	-0.3 (1)	0.16 (9)
O(3)	0.7080 (3)	0.5309 (2)	0.3930 (3)	3.1 (1)	3.0 (1)	3.6 (1)	-0.78 (9)	0.8 (1)	0.1 (1)
O(4)	0.4285 (3)	0.5634 (2)	0.2623 (3)	4.0 (1)	2.4 (1)	2.5 (1)	-0.75 (9)	0.01 (9)	0.02 (9)
O(5)	-0.1683 (3)	0.0112 (2)	0.1921 (3)	2.6 (1)	3.6 (1)	2.9 (1)	-0.90 (9)	0.59 (9)	-0.43 (9)
O(6)	0.1889 (3)	-0.0912 (2)	0.1073 (3)	2.6 (1)	2.8 (1)	3.8 (1)	-0.32 (9)	-0.4 (1)	0.4 (1)
O(7)	0.0318 (3)	0.0725 (2)	0.2383 (3)	2.9 (1)	3.3 (1)	2.6 (1)	-1.06 (9)	0.27 (9)	-0.44 (9)
O(8)	-0.0118 (3)	-0.1519 (2)	0.0610 (3)	3.0 (1)	2.4 (1)	3.6 (1)	-0.79 (9)	0.11 (9)	0.47 (9)
O(10)	0.4470 (3)	0.2730 (2)	0.5498 (3)	4.7 (1)	2.5 (1)	3.0 (1)	-1.4 (1)	0.7 (1)	0.09 (9)
O(20)	0.3069 (3)	0.0933 (2)	0.0542 (3)	2.9 (1)	4.4 (1)	4.0 (1)	-1.6 (1)	0.4 (1)	-1.0 (1)
C(1)	0.7416 (4)	0.4465 (3)	0.3943 (4)	2.9 (2)	3.8 (2)	2.6 (1)	-0.4 (1)	0.5 (1)	-0.4 (1)
C(2)	0.8883 (5)	0.4128 (4)	0.3389 (6)	3.6 (2)	5.4 (2)	4.9 (2)	0.3 (2)	1.1 (2)	0.2 (2)
C(3)	0.3898 (4)	0.4870 (3)	0.2277 (4)	2.9 (2)	2.8 (2)	2.6 (1)	-0.4 (1)	0.2 (1)	-0.1 (1)
C(4)	0.3189 (4)	0.4783 (3)	0.0686 (4)	4.0 (2)	3.6 (2)	2.6 (2)	-0.9 (2)	0.0 (1)	-0.1 (1)
C(5)	-0.0865 (4)	0.0546 (2)	0.2708 (4)	3.0 (2)	2.5 (1)	2.4 (1)	-0.2 (1)	0.2 (1)	0.0 (1)
C(6)	-0.1429 (4)	0.0951 (3)	0.4241 (5)	3.1 (2)	4.9 (2)	3.0 (2)	-0.3 (2)	0.4 (1)	-0.8 (2)
C(7)	0.1128 (4)	-0.1543 (3)	0.1043 (4)	2.8 (2)	2.9 (2)	2.7 (1)	0.0 (1)	0.2 (1)	0.0 (1)
C(8)	0.1828 (5)	-0.2468 (3)	0.1541 (5)	4.2 (2)	3.0 (2)	4.1 (2)	0.2 (2)	0.1 (2)	0.3 (2)
C(10)	0.4544 (6)	0.1182 (3)	0.6945 (6)	7.6 (3)	3.4 (2)	6.3 (3)	-1.2 (2)	1.4 (2)	1.3 (2)
C(11)	0.2272 (6)	0.2426 (5)	0.7011 (8)	4.6 (2)	8.1 (3)	9.6 (4)	-1.6 (2)	2.2 (2)	2.6 (3)
C(20)	0.5020 (5)	0.1811 (4)	0.1729 (7)	3.7 (2)	6.3 (3)	6.7 (3)	-2.1 (2)	-0.4 (2)	-1.2 (2)
C(21)	0.2326 (5)	0.2373 (3)	0.2344 (6)	4.5 (2)	4.2 (2)	6.2 (2)	-1.6 (2)	0.6 (2)	-1.6 (2)

atom	x	y	z	atom	x	y	z
D(101)	0.417 (5)	0.100 (3)	0.597 (6)	D(201)	0.559 (5)	0.132 (3)	0.148 (6)
D(102)	0.415 (5)	0.096 (4)	0.764 (6)	D(202) <sup>c</sup>	0.535	0.211	0.263
D(103)	0.563 (5)	0.108 (3)	0.702 (6)	D(203) <sup>c</sup>	0.490	0.223	0.090
D(111)	0.185 (5)	0.301 (4)	0.716 (6)	D(211)	0.265 (6)	0.278 (4)	0.301 (6)
D(112)	0.195 (5)	0.205 (4)	0.622 (6)	D(212)	0.133 (6)	0.216 (3)	0.268 (6)
D(113)	0.202 (5)	0.217 (4)	0.790 (6)	D(213)	0.245 (5)	0.272 (3)	0.153 (6)

<sup>a</sup> The form of the anisotropic thermal parameter is  $\exp[-1/4(B_{11}h^2a^{*2} + B_{22}k^2b^{*2} + B_{33}l^2c^{*2} + 2B_{12}hka^*b^* + 2B_{13}hla^*c^* + 2B_{23}klb^*c^*)]$ . <sup>b</sup> Deuterium atoms were assigned  $B_{\text{iso}} = 7.0 \text{ \AA}^2$ . <sup>c</sup> Calculated deuterium atom position.



**Figure 4.** Stereoview of the packing in  $\text{Rh}_2(\text{O}_2\text{CCF}_3)_4(\text{Me}_2\text{SO})_2$  showing the alignment of the dirhodium units. The thermal ellipsoids are drawn at the 20% probability level except the hydrogen atoms have been made arbitrarily small for clarity. The view is looking down the  $a$  axis with the  $b$  axis vertical and the  $c$  axis horizontal. The origin is in the upper front right corner.

size of  $\text{CD}_3$  is slightly less than that of  $\text{CH}_3$ .

It may well be that this "size" effect, essentially localized in the methyl groups themselves, is responsible for the different crystal structures of the protio and deuterio dirhodium com-

pounds we have studied. However, since the effect is so small on a "per methyl group" basis, and since the methyl groups constitute such a small fraction of the volume of  $\text{Rh}_2(\text{O}_2\text{CCF}_3)_4(\text{Me}_2\text{SO})_2$ , many aspects of what we have observed remain uncertain or obscure.

Doubtless, the two crystal structures must be of comparable though not exactly equal stability for both the protio and

(24) Anet, F. A. L.; Basus, V. J.; Hewett, A. P. W.; Saunders, M. J. *Am. Chem. Soc.* **1980**, *102*, 3945 and references therein.

